ISSN : 0974 - 7486 Volume 8 Issue 7

Trade Science Inc.

Materials Science

An Indian Journal

Full Paper

MSAIJ, 8(7), 2012 [271-279]

The infrared absorption and dielectric properties of manganese substituted lithium ferrite at room temperature

S.A.Mazen, N.I.Abu-Elsaad*

Magnetic Semiconductor Laboratory, Physics Department, Faculty of Science, Zagazig University, Zagazig, (EGYPT)

E-mail: nagwa.ibrahim@yahoo.com

Received: 26th January, 2012 ; Accepted: 26th February, 2012

ABSTRACT

Polycrystalline ferrites with general formula $Li_{0.5-0.5x}Mn_xFe_{2.5-0.5x}O_4$ (where x=0.0, 0.1, 0.3, 0.5, 0.7, 0.9 and 1.0) have been prepared by the ceramic method. The IR spectra have been reported in the range from 200 to 1000 cm^{-1}. The two primary bands corresponding to tetrahedral υ_A and octahedral υ_B were observed around 575 cm^{-1} and 370 cm^{-1}, respectively. Elastic properties of these mixed ferrites have been estimated as a function of composition. The values of Young's modulus (E), rigidity modulus (G), bulk modulus (B), Debye temperature (θ_D) and mean sound velocity (V_m) have been calculated from transverse (V_t) and longitudinal (V_l) wave velocities. The variation of elastic moduli with composition has been interpreted in terms of binding forces between the atoms of spinel lattice. The a.c. conductivity $\breve{\sigma}$ and dielectric properties (dielectric constant $\acute{\varepsilon}$ and dielectric loss ε" with loss tangent tan δ) were measured at room temperature as a function of frequencies from 10^2 to 10^6 Hz. The electrical conduction mechanism was explained in terms of the electron hopping model. The frequency exponential factor (s) was estimated and it was found to vary between 0.4 and 0.8.

KEYWORDS

IR;
Elastic behavior;
Dielectric properties;
Li-Mn ferrite.

INTRODUCTION

The polycrystalline ferrites have very important structural, magnetic, electrical and dielectric properties are dependent on several factors such as method of preparation, substitution of cations and microstructure, etc.[1,2]. Introduction of a relatively small amount of foreign ions can change the properties of the ferrites[3]. These changes can provide us information about the kind and amount of impurity required for obtaining a high-quality ferrite for any particular application. The modification in electric and magnetic properties of lithium ferrites by substitution of different ions has been studied by many investigators[4-6].

Infrared spectroscopy was used to determine the local symmetry in crystalline and non-crystalline solids and also to study the ordering phenomenon in ferrites[6]. The IR absorption bands mainly appear due to vibrations of oxygen ions with cations producing various frequencies of the unit cell. The frequencies depend upon cation masses, lattice parameter and cation–oxygen bonding, etc[7].

Full Paper

The ultrasonic pulse transmission technique (UPT) is the most common technique for elastic constants. However, a new technique based on the infrared spectroscopy has been developed by K.B Modi et al.[8] for studying the elastic properties of spinel ferrite and garnet systems. The elastic constants are of much importance because they reveal the nature of binding forces in solids and to understand the thermal properties of the solids[9]. The elastic properties of ferrites possessing the spinel structure have not been studied so systematically as their magnetic and electrical properties. Moreover, there is a need for a thorough study of the elastic behaviour of these ferrites with new compositions possessing certain desired elastic properties.

The present work is an attempt to estimate the elastic properties using the IR technique for Li-Mn ferrite. Also, the dielectric properties were investigated for the same composition at room temperature.

EXPERIMENTAL TECHNIQUES

Polycrystalline mixed Li–Mn ferrites having the chemical formula $Li_{0.5-0.5x}Mn_xFe_{2.5-0.5x}O_4$; 0.0=x=1.0 were prepared by the standard sintering ceramic method. The details of the method of preparation were explained in several previous publications[4,10]. IR spectra in the range from 200 to 1000 cm^{-1} were recorded at room temperature using the infrared spectrometer, (model 1430, PerkinElmer). The dielectric measurements were made at room temperature in the range of frequency from 100Hz up to 1MHz using RLC (Model PM6306 FLUKA). The measurements of dielectric constant (ε), dielectric loss (ε") and loss tangent (tan δ) of the ferrite samples were carried out on samples in disk shape of dimension 13mm diameter, and 3–5mm thickness using silver past as a contact. More details about the dielectric measurements were published in previous work[4,11].

RESULTS AND DISCUSSION

IR - analysis

The IR spectra of the above investigated composition $Li_{0.5-0.5x}Mn_xFe_{2.5-0.5x}O_4$ recorded in the range 200 – 1000 cm^{-1} is shown in Figure 1, and the absorption bands are summarized in TABLE 1. No absorption bands were observed above 1000 cm^{-1}. The IR spectrum of pure Li ferrite (x=0.0) has been analyzed in detail by Mazen et al.[12]. From the obtained spectra as shown in Figure 1, it is noticed that the primary band υ_1* and the second absorption band υ_2* are found to be in the range (585-546 cm^{-1}) and (379-372 cm^{-1}), respectively. The values of ν_1* are higher than that of ν_2* indicating that the normal mode of vibration of the tetrahedral complexes is higher than that of the corresponding octahedral site. This may be due to the shorter bond length of the tetrahedral site (R_A=1.89 Å) than that of the octahedral site (R_B=1.99Å)[13]. From TABLE 1 it is obvious that by introducing Mn^{2+} ions; the band υ_1* shifts slightly towards the lower frequency meanwhile the band υ_2* has no shift or change with frequency.

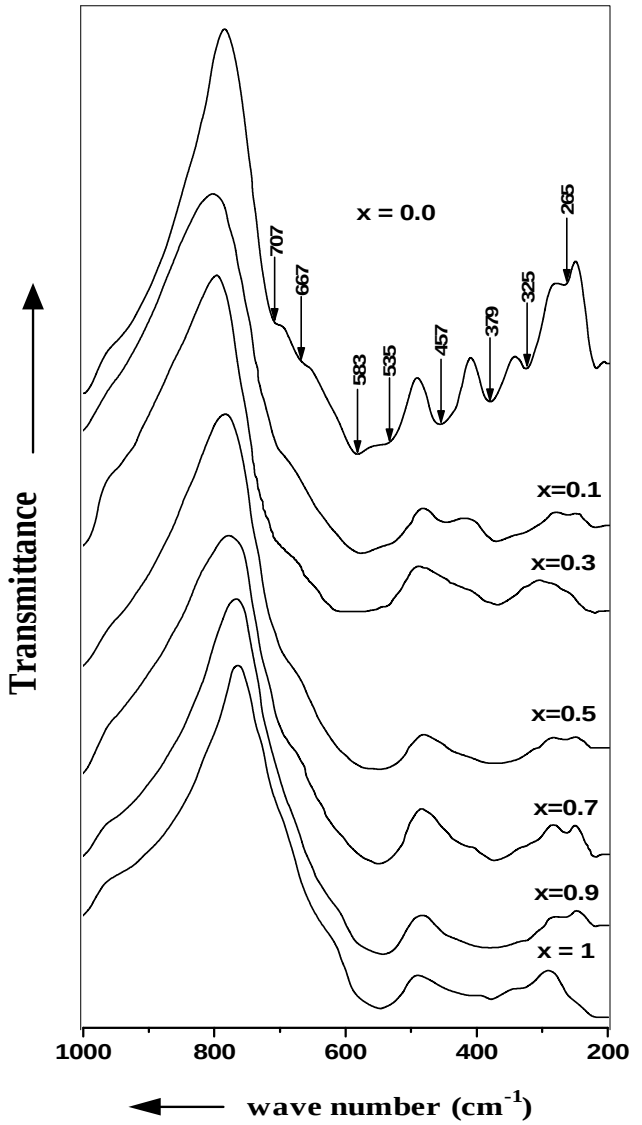

Figure 1 : IR absorption spectra of the mixed Li-Mn ferrites.

TABLE 1 : The IR absorption bands

x	Tetrahedral site (A-site)				Octahedral site (B-site)			
	$\upsilon_1(1)$	$\upsilon_1(2)$	υ_1^*	$\upsilon_1(3)$	$\upsilon_2(1)$	υ_2^*	υ_3	υ_4
0.0	707	667	585	543	457	379	325	267
0.1	704	-	578	530	450	375	330 ^{w}	265
	(w, sh)			(w, sh)				
0.3	-	-	584		-	372	327 ^{w}	267
0.5	-	-	557	-	-	374	310 ^{w}	268
0.7	-	-	553	-	-	375	324 ^{w}	265
0.9	-	-	547	-	-	376	327 ^{w}	265
1	-	-	546	-	-	376	325 ^{w}	-

***: The primary band, w: weak and sh: shoulder**

The third band υ_3 appeared at 325 cm^{-1} for x=0.0 and changed to weak shoulder for x=0.1. This band could be attributed to divalent metal ion-oxygen complexes in octahedral sites. Hence, its appearence gives an indication to the presence of a small amount of Fe^{2+} ions in the above-mentioned compositions[14]. The fourth vibrational band υ_4 (around 265 cm^{-1}) is due to the lattice vibration[15].

The obtained spectum indicates splitting in the absorption bands, i.e., the first primary band (υ_1*) consist of two shoulders $\upsilon_1(1)$ at 710 and $\upsilon_1(2)$ at 670 cm^{-1} and another small band $\upsilon_1(3)$ at 535 cm^{-1}. It has been shown by Potakova et al.[16] that the the presence of Fe^{2+} ions in ferrites can produce splitting of or shoulders on absorption bands. This is attributed to the Jahn-Teller distortion produced by the Fe^{2+} ions, which cause local deformations in the crystal field potential, and hence lead to the splitting of the band υ_1. These bands have been appeared in the samples (with x=0.0 and 0.1) then completly disappeared at high concentration of manganese.

According to Tarte[17] and Mazen et al.[12], the high frequency band $\nu_2(1)$ recorded only for x=0.0 and x=0.1 in the range (450-458 cm^{-1}) could be assigned to Li^+-O^{2-} complexes on octahedral site. The intensity of this band goes on decreasing with the increase x since the Li^+ content decreases with increasing x, so it persists only up to x=0.1. Then it completely disappeared for x=0.3.

The threshold frequency υ_{th} for the electronic transition can be determined from the maximum point of absorption spectra where it reaches a limiting value[18]. These threshold values are illustrated in Figure 2. It is found that the threshold frequency (υ_{th}) decreases with increasing Mn content for x = 0.1; that is, with decreasing both Fe^{3+} and Li^+ concentration.

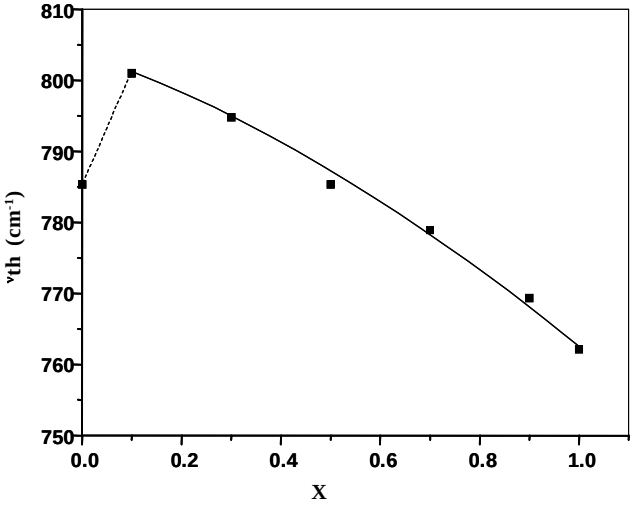

Figure 2 : The dependence of threshold frequency ν_{th} with composition x.

The force constant was calculated for tetrahedral site (k_t) and octahedral site (k_o) using the method suggested by Waldron[18]:

$$\mathbf{K_t = 7.62 \times M_A \times \upsilon_1^2 \times 10^{-7}\ N/m} \quad (1)$$

$$\mathbf{K_o = 10.62 \times M_B / 2 \times \upsilon_2^2 \times 10^{-7}\ N/m} \quad (2)$$

where M_A and M_B are the molecular weights of cations on A- and B-sites, respectively. Both M_A and M_B were calculated from the cation distribution formula suggested in TABLE 2. The calculated values of the force constants K_t and K_o are listed in TABLE 3 and presented in Figure 3. It can be seen that, K_t decreases while K_o increases with increasing Mn content. Furthermore the calculated values of K_t are greater than that of the corresponding values of K_o. However the values of the bond length of A- site (R_A) are smaller than that of B site (R_B) as mentioned before. This is due to the inverse proportionality between the bond length and the force constants[19].

TABLE 2 : The cation distribution of Li-Mn ferrite samples (with 0.0=x=1.0).

X	Cation distribution
0.0	$\left(Fe^{3+}\right)^A\left[Li^+_{0.5}Fe^{3+}_{1.5}\right]^B O_4^{2-}$
$0.1 \le x \le 0.5$	$\left(Fe^{3+}_{1-x}Mn^{2+}_{x}\right)\left[Li^+_{0.5-0.5x}Fe^{3+}_{1.5+0.5x}\right]O_4^{2-}$
$0.5 < x \le 1.0$	$\left(Fe^{3+}_{1-x+y}Mn^{2+}_{x-y}\right)\left[Li^+_{0.5-0.5x}Mn_yFe^{3+}_{1.5+0.5x-y}\right]O_4^{2-}$

( )^A: A-site and [ ]^B: B-site.

Full Paper

TABLE 3 : The force constants and elastic constants calculated for Li-Mn ferrite samples

x	K_t	K_o	V_L	V_t	B	E	G	P	V_m	V_A	Θ'_D	Θ_D
	(N/m)		(m/s)		GPa				m/s	($10^{-6}m^3$)	K	K
0.0	145.41	66.54	5171	2985	127.22	114.49	42.41	0.35	3314	6.22	454	693
0.1	142.03	66.97	5119	2956	125.22	112.7	41.74	0.35	3281	6.26	448	685
0.3	144.35	69.62	5137	2965	127.82	115.04	42.61	0.35	3293	6.32	448	687
0.5	130.78	74.01	4982	2876	121.89	109.71	40.63	0.35	3193	6.37	434	669
0.7	128.83	78.04	4969	2869	122.69	110.43	40.89	0.35	3186	6.43	431	668
0.9	125.44	82.06	4943	2853	122.78	110.51	40.93	0.35	3168	6.49	428	664
1.0	124.87	83.85	4961	2864	122.78	110.49	40.93	0.35	3179	6.61	427	663

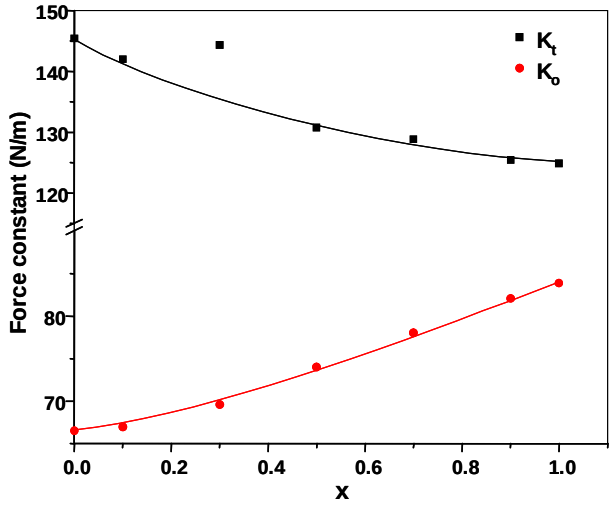

Figure 3 : The variation of force constant K with composition x.

From IR spectra, the values of half bandwidth for each site are calculated and the ratio Γ_A/Γ_B is represented in Figure 4. It can be noticed that the ratio Γ_A/Γ_B decreases with the increase in Mn content. The half bandwidth depends on the statistical distribution of various cations over the two sites[14]. This dependence is related to the replacement process that occur between smaller ionic radius Fe^{3+} (0.064 nm) and Li^{+} (0.073 nm) with larger ionic raduis Mn^{2+} (0.08 nm).

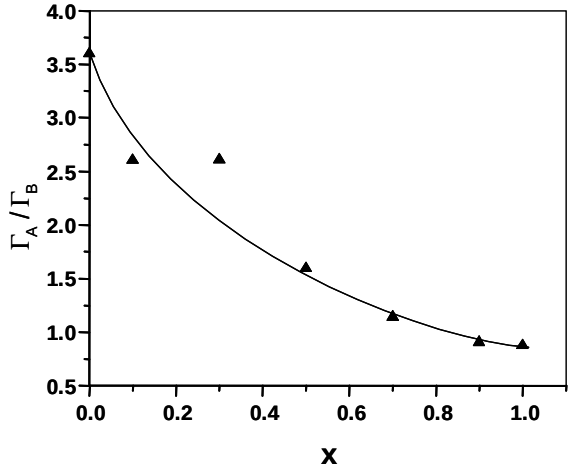

Figure 4 : Change in half band width ratio (Γ_A/Γ_B) against composition x

The Debye temperature θ_D was calculated by using the following relation[18]:

$$\theta_D = \frac{\hbar C v_{av}}{k} \quad (3)$$

where, $v_{av} = \frac{v_A + v_B}{2}$, v_A is the frequency of the primary band of A-site, v_B is the frequency of the primary band of B-site, h = h/2π, *h* is the Plank constant, k is the Boltzmann's constant and C =3×10[10] cm/s; is the velocity of light. The calculated values of the Debye temperature are tabulated in TABLE 3. It can be noticed that all values of the Debye temperature are varying between 660 and 690K. These values have a great importance to determine the conduction mechanism of these compositions. It can be seen that θ_D decreases with increasing Mn concentration. This behaviour can be discussed on the basis of specific heat theory. According to this theory, electrons absorbed part of the heat and θ_D may decrease with increasing Mn concentration, this suggests that the conduction for these samples due to electrons (i.e. n-type)[20].

Elastic properties

To study the elastic properties of spinel ferrite and garnet systems a new technique based on the infrared spectroscopy has been developed by K.B Modi et al.[8]. The different elastic modulii can be evaluated using the following relations:

The bulk modulus (*B*) of solids is defined as:

$$B = 1/3[C_{11} + 2C_{12}], \quad (4)$$

where C_{11} and C_{12} are the stiffness constants. But according to Waldron et al.[18] for isotropic materials with

cubic symmetry like spinel ferrites and garnets, C_{11}~C_{12}, therefore, $B = C_{11}$. Also, the force constant (k) is related to the stiffness constant by [$k=aC_{11}$][21], where k is the average force constant ($k=(k_t + k_o)/2$). Further, the values of the longitudinal elastic wave (V_l) and the transverse elastic wave (V_t) have been determined as follows[22,23]:

$$V_l = (C_{11}/d_x)^{1/2} \text{ and } V_t = \frac{V_l}{\sqrt{3}} \quad (5)$$

The variation of the sound velocity longitudinal (V_l) and transverse (V_t) as a function of Mn composition x is depicted in TABLE 3. It can be seen that both the velocity (V_l and V_t) decrease with substitution of Mn. The values of V_l and V_t are used to calculate the elastic moduli of the ferrite specimens using the following formulae[24]:

$$\text{Mean elastic wave velocity } V_m = \frac{1}{3}\left[\frac{2}{V_l^2} + \frac{1}{V_t^2}\right]^{-1/3} \quad (6)$$

$$\text{Rigidity modulus (G)} = d_x V_t^2 \quad (7)$$

$$\text{Poisson's ratio (P)} = 3B - 2G / 6B + 2G \quad (8)$$

$$\text{Young's modulus (E)} = (1 + P)2G \quad (9)$$

The calculated values of different elastic moduli for the investigated composition Li-Mn ferrite are reported in TABLE 3. From this table, it can be seen that, B, E and G slightly decrease with increasing Mn-content (x). Figure 5 shows the variation of bulk modulus (B) and Young's modulus (E) with Mn substitution. According to Wooster work[22] the behaviour of elastic moduli is attributed to the strengthening of the inter-atomic binding between various atoms of the spinel lattice with increasing Mn ion content. The inter-atomic binding between various atoms is getting weakened continuously and therefore elastic moduli decrease with manganese content x. Similar results have been observed in the case of Ni–Zn ferrite[25] and Co-Zn ferrite[26] wherein the inter-atomic binding between the various atoms decreases with increasing Zn content x.

The Debye temperature θ'_D was calculated employing Anderson's formula[27]:

$$\theta'_D = \frac{h}{k_B}\left[\frac{3N_A}{4\pi V_A}\right]^{1/3} .V_m \quad (10)$$

where, V_A is mean atomic volume given by $(M/d_x)/q$, M the molecular weight, q is the number of atoms in the formula unit (i.e. 7) and N_A, is Avogadro's number. The calculated values are listed in TABLE 3. It is observed that the Debye temperature θ_D calculated according to Waldron is higher than that calculated according to Anderson's formula θ'_D but both of them decrease with increasing manganese substitution.

A plot of average sound velocity (V_m) against Debye temperature (θ'_D) is shown in Figure 6. It is interesting to note from the figure that the average sound velocity increases linearly with the Debye temperature. A similar variation was also reported by Reddy[28] in the case of Mn–Mg mixed ferrites and by Ravinder[9] in the case of Li-Mn mixed ferrites. This behaviour clearly indicates the direct relationship between the acoustic pa-

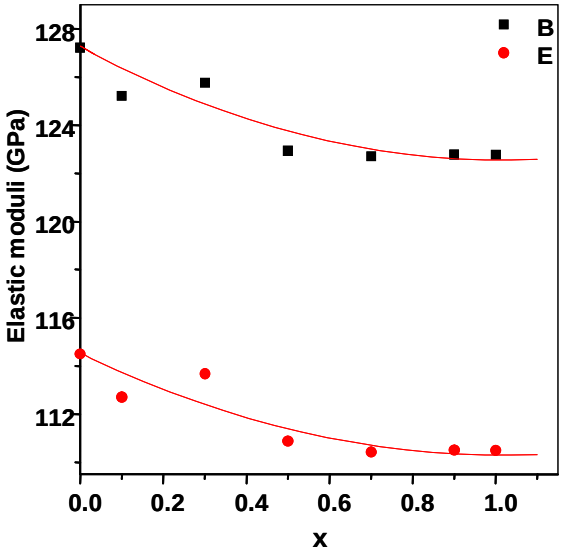

Figure 5 : Variation of both bulk and young moduli with composition x for the system $Li_{0.5-0.5x}Mn_xFe_{2.5-0.5x}O_4$.

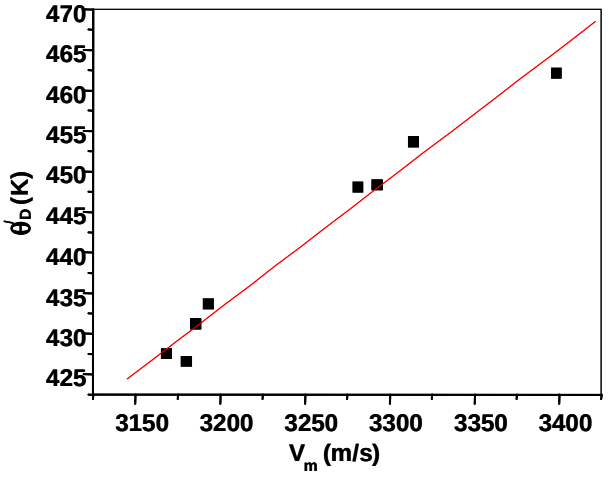

Figure 6 : Plot of debye temperature θ'_D against average sound velocity V_m.

rameter (average sound velocity) and the important thermodynamic parameter (Debye temperature).

Effect of frequency on dielectric properties

The AC conductivity $\tilde{\sigma}$ with the dielectric properties (dielectric constant ε' and dielectric loss ε") as a function of frequency (f = 10^2-10^6Hz) at RT for the above mentioned composition are shown in Figure 7, while Figure 8 shows the variation of loss tangent (tan δ) for x=0.0, 0.5 and 1.0, respectively (as examples). The AC conductivity shows dispersion with respect to

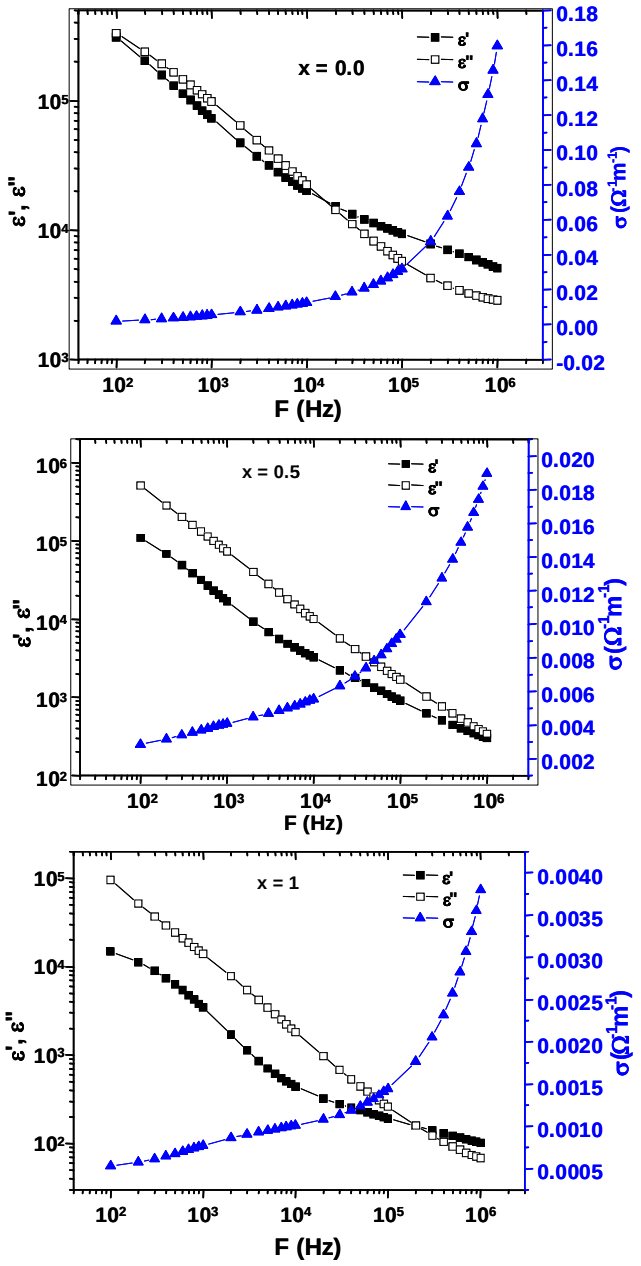

Figure 7 : Plots of ε', ε" and σ versus frequency at room temperature for x = 0.0, 0.5 and 1.

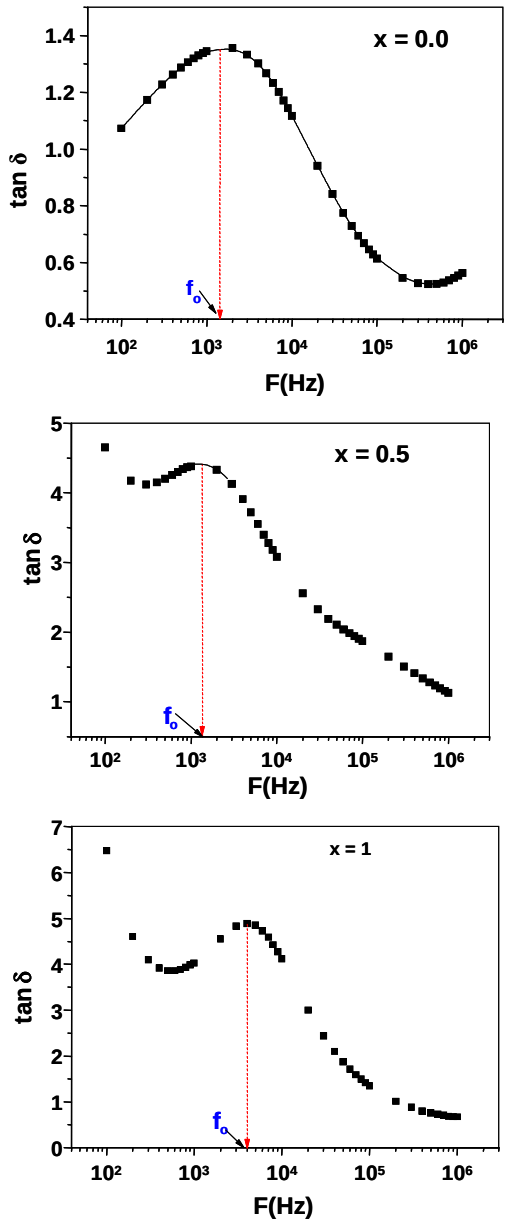

Figure 8 : Variation of the dielectric loss tangent (tan δ) with frequency at room temperature for x = 0.0, 0.5 and 1.

frequency. It increases slowly at lower frequencies, but after a certain frequency (≈10^4 Hz) it increases rapidly until it reaches a maximum value. The dispersion in $\tilde{\sigma}$ with frequency has been explained by Koop's theorem[29], which supposed that the ferrite compact acts as a multilayer capacitor. In this model, the ferrite grain and grain boundaries have different properties. The effect of the multilayer condenser rises with frequency; as a result the conductivity increases. The conductivity is a complex quantity[30]:

$$\tilde{\sigma} = \sigma' + i\sigma'' \quad (11)$$

whose real and imaginary components are:

$$\sigma' = \frac{\sigma_o}{1+\omega^2\tau^2}, \quad \sigma'' = \frac{\sigma_o\omega\tau}{1+\omega^2\tau^2} \qquad (12)$$

In the low frequency region, $\omega\tau << 1$, $\sigma'' << \sigma'$. That is, the electrons exhibit an essentially resistive character. In the high frequency region, $\omega\tau >> 1$, $\sigma'' >> \sigma'$, the electrons evince an essentially inductive character. The electrical conduction mechanism can be explained in terms of the electron hopping model by Heikes and Johnson[31]. In other words, the conduction mechanism could be due to the electron hopping between two adjacent octahedral sites (B-sites) in the spinel lattice and a transition between $Fe^{2+} \leftrightarrow Fe^{3+}$ ions or $Mn^{2+} \leftrightarrow Mn^{3+}$ might take place[32]. Thus by the electronic exchange, one obtains local displacement of electrons in the direction of the applied electric field.

The complex dielectric constant ε^* is representing by[30]:

$$\varepsilon^* = \varepsilon' - j\,\varepsilon''; \qquad (13)$$

where έ describes the stored energy while ε" describes the dissipated energy. The behaviour of both ε' and ε" against frequency at room temperature are shown in Figure 7. The general trend for all compositions is that ε' and ε" decrease with increasing frequency. However, ε" decreases faster than ε' over the same range of frequency. In the high-frequency range the values of ε' become closer to the value of ε". All samples exhibit dispersion due to Maxwell interfacial polarization in agreement with phenomenological theory[29]. This behaviour of a dielectric may be explained qualitatively by the supposition that the mechanism of the polarization process in ferrite is similar to that of the conduction process. The electrical conduction mechanism can be explained by the electron hopping model of Heikes and Johnston[31]. The electron hopping ($Fe^{2+} \leftrightarrow Fe^{3+}$ or $Mn^{2+} \leftrightarrow Mn^{3+}$) occurs by electron transfer between adjacent octahedral sites (B-sites) in the spinel lattice[32]. Thus by the electronic exchange: $Fe^{2+} + Mn^{3+} \leftrightarrow Fe^{3+} + Mn^{2+}$.

One obtains local displacements of electrons in the direction of the applied electric field; these displacements determine the polarization of the ferrite. It is known that the effect of the polarization is to reduce the field inside the medium. Therefore, the dielectric constant of the substance may decreases substantially as the frequency is increased. Therefore, the dielectric constant of the substance may be decreased substantially as the frequency is increased. Also, such a decrease can be attributed to the fact that the electric exchange between Fe^{2+} and Fe^{3+} ions cannot follow the external applied field beyond a certain frequency.

Figure 8 shows the variation of loss tangent tan δ with frequency for the investigated composition. It is known that the loss tangent ($\tan\delta = \varepsilon''/\varepsilon'$). A maximum in tan δ at a certain frequency (f_o) can be observed when ε' has a minimum value i.e. a minimum stored energy at that frequency. Another explanation of the occurrence of peaks in the variation of loss tangent with frequency can be observed when the hopping frequency is approximately equal to that of the externally applied electric field; i.e., it means "resonance phenomenon". The condition for observing a maximum in tan δ of a dielectric material is given by the relaxation[33]:

$$\omega_o\,\tau = 1 \qquad (14)$$

where $\omega_o = 2\pi f_o$ and τ is the relaxation time. This relaxation time is related to the jumping (hopping) probability per unit time, p, by the equation:

$$\tau = \frac{1}{2p} \quad \text{or} \quad f_o \propto p \qquad (15)$$

This equation shows that f_o is proportional to the hopping probability. It was found that $\tau = 1.11\times10^{-4}$, 1.19×10^{-4} and 3.98×10^{-5} s for x = 0.0, 0.5 and 1.0, respectively.

Determination of the frequency exponential factor(s)

Because the hopping conduction mechanism was assumed in the above investigated system of Li-Mn ferrite, the AC conductivity $\tilde{\sigma}(\omega)$ can be represented by a power law[30]:

$$\tilde{\sigma}(\omega) \propto A\omega^s, \qquad (16)$$

where A is slightly dependent on temperature, ω is the applied frequency at which the conductivity $\tilde{\sigma}$ was measured and the powers, which is a weak function of frequency, is to be determined for the investigated composition where it is of the order of $(0.4 - 0.8)$[30]. Pike[34] and Elliot[35] have considered s = 1 and it expressed by the following relation[30,35]:

$$s = 1 - \frac{4}{\ln(\upsilon_{ph}/\omega)} \qquad (17)$$

In the present study of Li-Mn ferrite system, the values

Full Paper

of s were calculated from the relation log $\tilde{\sigma}$ versus log ω shown in Figure 9. This relation shows a straight line in the range of frequency from 10^4 Hz up to 1MHz. The estimated values of the power s were listed in TABLE 4. It is found that s- factor is composition dependent, where s decreases up to x = 0.5 by 55% and then increases by 35% with further increase in x.

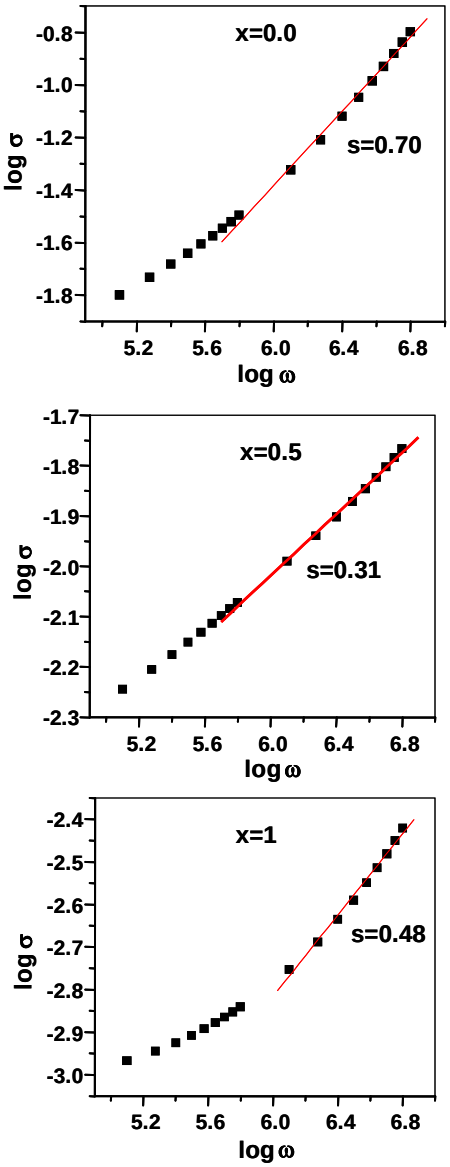

Figure 9 : Variation of the exponential factor (S) with angular frequency ω at room temperature for x=0.0, 0.5 and 1.

Also, the phonon frequency ν_{ph} for each composition of Li–Mn ferrite was calculated at f = 5 ×10^5 Hz and compared with those calculated from IR spectra[4]. The values of the phonon frequency were tabulated in TABLE 4. It was found that the values of ν_{ph} calculated from (log $\tilde{\sigma}$ - log ω) plots are lower than that calculated from IR absorption spectra by a factor of about 10^2–10^5 Hz (TABLE 4). This difference may be related to the nature of polarization in each case. In the AC field the polarization is due to ionic and electronic polarization, while in the IR spectra, the polarization is due to electronic polarization only. Also, the value of υ_{ph} (A-site) is bit higher than that of υ_{ph} (B-site). This may be due to the nature of bond in A-site which is characterized by covalent bond only, while the nature of B-site is characterized by ionic and covalent.

TABLE 4 : The calculated s-values and ν_{ph} for each composition

x	s	ν_{ph} (Hz) from (logω-logσ) plots	ν_{ph} (10^{13} Hz) from IR spectra	
			A-site	B-site
0.0	0.70	2.67×10^{12}	1.75	1.14
0.1	0.64	6.21×10^{11}	1.73	1.13
0.3	0.51	1.03×10^{10}	1.75	1.12
0.5	0.31	1.00×10^{9}	1.67	1.12
0.7	0.28	7.99×10^{8}	1.66	1.13
0.9	0.38	2.09×10^{9}	1.64	1.13
1.0	0.48	6.68×10^{9}	1.64	1.12

CONCLUSION

1 The IR spectra confirmed the formation of spinel structure and gave information about the distribution of ions between the two sites, tetrahedral (A-site) around 575 cm^{-1} and octahedral (B-site) around 370 cm^{-1}.

2 The behaviour of Debye temperature θ_D shows that the electrons should make a significant contribution to the specific heat.

3 The elastic modili bulk modulus (B) and Young's modulus (E) are dependent on Mn concentration in Li-Mn ferrite.

4 From the a.c. conductivity measurements and consequently the dielectric properties (έ and ε") can be concluded that the obtained results are explained in terms of the hopping model where an electronic exchange of the form Fe^{2+}+ Mn^{3+} ↔ Fe^{3+}+ Mn^{2+}.

5 The phonon frequency υ_{ph} which calculated from IR spectra was found to be higher than that calculated from the AC conductivity by a factor of about 10^2 - 10^5 Hz and this may be due to the nature of polarization in each case.

REFERENCES

[1] P.P.Hankare, R.P.Patil, U.B.Sankpal, S.D.Jadhav, I.S.Mulla, K.M.Jadhav, B.K.Chougule; J.of Mag.and Mag.Mater., **321**, 3270 **(2009)**.

[2] E.Wolska, K.Stempin, O.Krasnowska-Hobbs; Solid State Ionics, **101**, 527 **(1997)**.

[3] A.Y.Lipare, P.N.Vasambekar, A.S.Vaingankar; Phys.Status Solidi (a), **2**, 372 **(2003)**.

[4] S.A.Mazen, S.F.Mansour, E.Dhahri, H.M.Zaki, T.A.Elmosalami; J.of Alloys and Compds., **470**, 294-300 **(2009)**.

[5] Tatsuya Nakamura, Hiroyuki Demidzu, Yoshihiro Yamada; J.of Phys.and Chem.of Sol., **69**, 2349-2355 **(2008)**.

[6] P.P.Hankare, et al.; J.of Mag.and Mag.Mater., **321**, 3270-3273 **(2009)**.

[7] A.M.Shaikh, S.A.Jadhav, S.C.Watawe, B.K.Chougule; Mater.Lett., **44**, 192-196 **(2000)**.

[8] K.B.Modi, U.N.Trivedi, M.P.Pandya, S.S.Bhatu, M.C.Chhantbar, H.H.Joshi; Microwaves and Optoelectronics. Anamaya Publishers, New Delhi, 223 **(2004)**.

[9] D.Ravinder, L.Balachander, Y.C.Venudhar; Materials Letters, **49**, 205 **(2001)**.

[10] S.A.Mazen; J.Mater.Chem.and Phys., **62**, 139 **(2000)**.

[11] S.A.Mazen, A.M.El Taher; J.Alloys and Compd., **498**, 19-25 **(2010)**.

[12] S.A.Mazen, M.H.Abdallah, R.I.Nakhla, F.Metawe, H.M.Zaki; Mater.Chem.and Phys., **34**, 35 **(1993)**.

[13] B.J.Evans, S.Hafner; J.Phys.and Chem.Solids, **29**, 1573 **(1968)**.

[14] S.A.Mazen, F.Metawe, S.F.Mansour; J.Phys.D: Appl.Phys., **30**, 1799-1808 **(1997)**.

[15] O.S.Josylu, J.Sobhanadri; Physica Status Solidi (a), **65**, 479 **(1981)**.

[16] V.A.Potakova, N.D.Zverv, V.P.Romanov; Phys. Stat.Sol.(a), **12**, 623 **(1972)**.

[17] P.Tarte; Acta Crystallogr., **16**, 228 **(1963)**.

[18] R.D.Waldron; Phys.Rev., **99**, 1727 **(1955)**.

[19] S.C.Watawe, B.D.Sutar, B.D.Sarwade, B.K.Choguleu; International J.of Inorganic Mater., **3**, 819 **(2001)**.

[20] S.A.Mazen, A.M.Abdel-Daiem; J.Mat.Chem.and Phys., (Corrected proof).

[21] S.L.Kakani, C.A.Hemrajani; Text Book of Solid State Physics, 3rd Edition, Sultan Chand & Sons, New Delhi, 150 and 190 **(1997)**.

[22] W.A.Wooster; Rep.Prog.Phys., **16**, 62 **(1953)**.

[23] D.Ravinder, T.Manga; Mater.Lett., **41**, 254 **(1999)**.

[24] B.Raj, V.Rajendram, P.Palanichamy; Science and Technology of Ultrasonics, Narosa Pub. House, New Delhi, **250**, **(2004)**.

[25] S.Srinivas Rao, D.Ravinder; Mater.Lett., **57**, 3802 **(2003)**.

[26] V.G.Patil, Sagar E.Shirsath, S.D.More, S.J.Shukla, K.M.Jadhav; J.of Alloys and Compd., **488**, 199 **(2009)**.

[27] O.L.Anderson; Physical Acoustics III B, Academic Press, New York, 43 **(1965)**.

[28] P.V.Reddy; Phys.Status Solidi A, **108**, 607 **(1988)**.

[29] C.G.Koops; Phys.Rev., **83**, 121 **(1951)**.

[30] N.F.Mott, E.A.Davis; Electronic Processes in Non-CrystallineMaterials, Claren-don Press, Oxford, Great Britain, **(1979)**.

[31] R.R.Heikes, W.D.Jonston; J.Chem.Phys., **26**, 582 **(1957)**.

[32] G.H.Jonker; J.Phys.Chem.Solids, **9**, 105 **(1959)**.

[33] M.B.Reddy, P.V.Reddy; J.Phys.D: Appl.Phys., **24**, 975 **(1991)**.

[34] G.F.Pike; Phys.Rev.B, **1572**, 6 **(1972)**.

[35] S.R.Elliott; Phill.Mag., **36**, 1291 **(1977)**.